PROCEEDINGS OF SPIE

SPIEDigitalLibrary.org/conference-proceedings-of-spie

Volumetric photoacoustic endoscopy of upper gastrointestinal tract: ultrasonic transducer technology development

Joon-Mo Yang, Christopher Favazza, Ruimin Chen, Konstantin Maslov, Xin Cai, et al.

Joon-Mo Yang, Christopher Favazza, Ruimin Chen, Konstantin Maslov, Xin Cai, Qifa Zhou, K. Kirk Shung, Lihong V. Wang, "Volumetric photoacoustic endoscopy of upper gastrointestinal tract: ultrasonic transducer technology development," Proc. SPIE 7899, Photons Plus Ultrasound: Imaging and Sensing 2011, 78990D (17 February 2011); doi: 10.1117/12.875377

SPIE.

Event: SPIE BiOS, 2011, San Francisco, California, United States

Volumetric photoacoustic endoscopy of upper gastrointestinal tract: ultrasonic transducer technology development

Joon-Mo Yang[1], Christopher Favazza[1], Ruimin Chen[2], Konstantin Maslov[1], Xin Cai[1], Qifa Zhou[2], K. Kirk Shung[2], and Lihong V. Wang[1*]

[1]Optical Imaging Laboratory, Department of Biomedical Engineering, Washington University in St. Louis, One Brookings Drive, Campus Box 1097, St. Louis, Missouri, 63130, USA

[2]Ultrasonic Transducer Resource Center, Department of Biomedical Engineering, University of Southern California, 1042 Downey Way, University Park, DRB 130, Los Angeles, CA 90089, USA

ABSTRACT

We have successfully implemented a focused ultrasonic transducer for photoacoustic endoscopy. The photoacoustic endoscopic probe's ultrasound transducer determines the lateral resolution of the system. By using a focused ultrasonic transducer, we significantly improved the endoscope's spatial resolution and signal-to-noise ratio. This paper describes the technical details of the ultrasonic transducer incorporated into the photoacoustic endoscopic probe and the experimental results from which the transducer's resolution is quantified and the image improvement is validated.

Keywords: Photoacoustic endoscopy, volumetric imaging, tomography, focused ultrasonic transducer, gastrointestinal tract.

1. INTRODUCTION

Photoacoustic endoscopy (PAE)[1-3] is a novel technology that embodies photoacoustic tomography[1,4-6] in a small probe that can be used for minimally invasive imaging. PAE can provide microscopic or macroscopic depth-resolved cross-sectional and volumetric images of target tissues[2,3]. With its unique optical-absorption-based image contrast, PAE compares favorably to other existing endoscopic imaging modalities, such as endoscopic ultrasound (EUS)[7,8], endoscopic optical coherence tomography (OCT)[9,10] or confocal endoscopy[11]. Although OCT and confocal imaging provide cellular level (~μm) image resolution for diseased tissues *in vivo*, these techniques are limited by their inability to penetrate deep tissues because they rely on unscattered, ballistic photons. EUS, which is a representative clinically-translated and deeply-penetrating endoscopic modality, suffers from speckle artifacts and poor image contrast. Conversely, PAE can produce images with high acoustic resolution and optical-absorption based contrast at depths far beyond the quasi-ballistic photon regime[2-4]. The high optical absorption-based contrast and depth-resolved image production is attributed to its signal excitation mechanism which utilizes laser pulses instead of mechanical pulses to generate photoacoustic (PA) waves. By simply changing the laser wavelength, rich spectroscopic image information of target tissue can be acquired, which enables quantitative assessment of functional information (e.g., Hb concentration, sO_2).

In 2009 and 2010, our group reported a PA endoscope prototype which integrated all necessary units, including a light illumination unit, an ultrasound detection unit, and a mechanical scanning unit, into a single probe and enabled *in situ* PA endoscopic imaging of an intact gastrointestinal tract of a rat[2,3]. One of important features of the imaging probe was its built-in scanning mirror-based actuator housed at the distal end of the probe, which enabled static mounting of the associated illumination and ultrasound pulse generation-detection units. This built-in scanning mechanism yields

* Corresponding author: lhwang@biomed.wustl.edu

Photons Plus Ultrasound: Imaging and Sensing 2011, edited by Alexander A. Oraevsky, Lihong V. Wang,
Proc. of SPIE Vol. 7899, 78990D · © 2011 SPIE · CCC code: 1605-7422/11/$18 · doi: 10.1117/12.875377

higher-quality images because mechanical scanning is much more stable than the conventional, flexible-shaft-based, proximal-actuation method. This prototype[2,3], however, possessed poor image spatial resolution, especially lateral resolution, which was primarily limited by the PA signal detection unit that utilized an unfocused transducer (2.0 mm aperture, 40 MHz $LiNbO_3$). In this study, we substantially improved the endoscope's image resolution by employing a focused transducer with a high acoustic numerical aperture. The focused transducer-based endoscopic probe enabled three-dimensional visualization of blood vasculature with high spatial resolution. Here, we describe technical details of the implemented ultrasonic transducer and experimental results obtained to quantify the transducer's resolution and to validate the image quality improvement.

2. MATERIALS AND METHOD

2.1. Design and fabrication of the focused ultrasonic transducer

The ultrasonic transducer determines the image resolution of PA endoscope in the diffusive optical regime, particularly relevant when imaging highly scattering biological tissues. Employing a focused transducer could improve the overall image quality, especially transverse resolution, and signal-to-noise ratio. In this study, we fabricated a focused transducer by forming a plano-concave-shaped plastic acoustic lens and fixing it to the flat surface of the transducer's piezo-element. The plastic acoustic lens was fabricated by molding a liquid plastic.

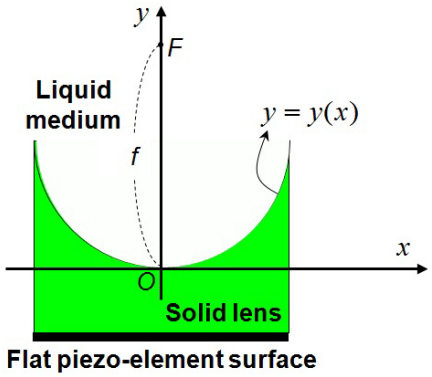

Figure 1. Definition of coordinate system for a plano-concave lens: *F*, focal point; *O*, origin; *f*, focal distance.

In the case of the plano-concave shaped lens as shown in **Figure 1**, the concave surface's ideal curve, i.e., y(x), without geometric acoustic aberration is expressed by the following ellipsoidal form for a given focal distance *f*. [12]

$$y(x) = b(1-\sqrt{1-x^2/a^2}), \text{ where } a \equiv f\sqrt{(n-1)/(n+1)}, \quad b \equiv f \cdot n/(1+n)$$

Here, n is the acoustic speed ratio of the solid lens to the surrounding liquid medium (water in this study) for the longitudinal waves. This formula implies that the transducer's aperture should be less than 2*a* to receive acoustic waves without aberration and the curve shape approaches the spherical form only if the acoustic speed ratio is sufficiently high (n>>1).

In this study, $LiNbO_3$ crystal and polyester were used to form the ultrasonic transducer's piezo-element and the acoustic lens materials, respectively, and their acoustic properties[13] are shown in Table 1.

Table 1. Acoustic properties of materials.

	$LiNbO_3$	Polyester	Water
Longitudinal wave speed (mm/μs)	7.34	2.49	1.48
Acoustic impedance (MRayls)	34.1	3.04	1.48

Considering our endoscopic probe's internal geometry and diameter (OD: 3.8 mm), we targeted a 2.6 mm aperture and a focal distance of around 5 mm for our transducer. For a 5 mm focal distance, the formula yields the values of a=2.52 mm and b=3.14 mm, based on the acoustic speed ratio (n=1.68) shown in **Table 1**. In **Figure 2**, we present the ideal shape of the lens drawn in the same scale for the horizontal and vertical directions. Since the fabrication of such ellipsoidal lens is relatively challenging and expensive, we formed a simple spherical lens that most closely matched the ellipsoidal shape. The spherical lens's radius of curvature was determined by a curve fitting method as shown in **Figure 2**.

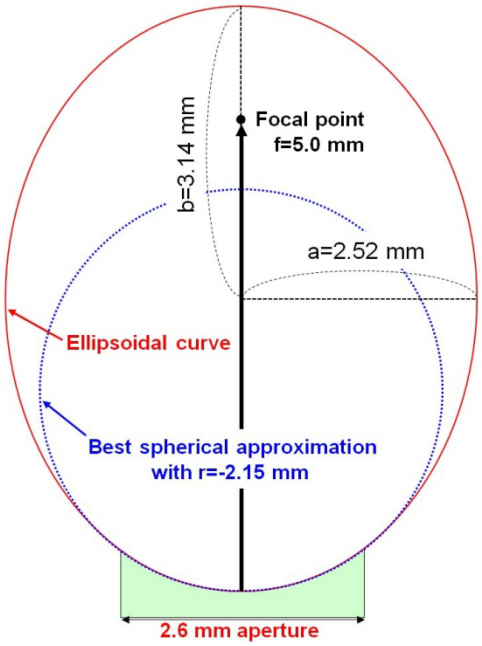

Figure 2. Illustration of spherical curve fitting to the front surface of the ideal ellipsoidal lens having a longer-half-axis b of 3.14 mm and shorter-half-axis a of 2.52 mm, which yields a focal distance of 5.0 mm.

In the actual lens fabrication, we chose a 2.18 mm radius of curvature because this value was the most suitable size to yield the target focal distance of around 5 mm, considering the available sizes of metal ball bearings used in the molding process. With a 2.18 mm radius of curvature, the expected focal distance is approximately 5.1 mm, based on the spherical curve fitting method (**Fig. 2**) over the entire aperture of 2.6 mm. We chose the edge and center thickness of transducer to be ~0.8 mm and ~0.2 mm, respectively, to minimize the acoustic attenuation of high frequency acoustic waves. With these dimensions, we molded a plano-concave shaped plastic acoustic lens and attached it to the flat piezo-element surface. **Figure 3** shows the structure and implemented shape of the transducer.

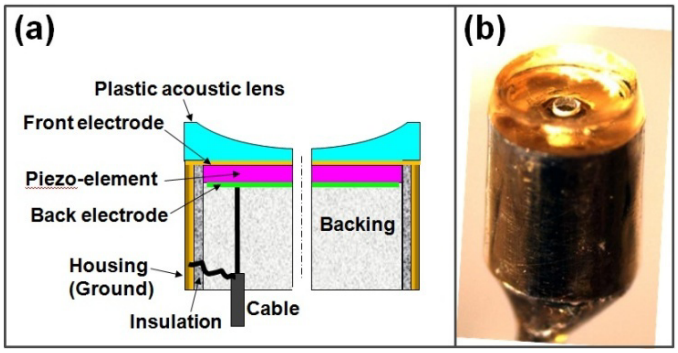

Figure 3. Schematics **(a)** and picture **(b)** of the focused transducer.

The experimentally measured focal distance of the fabricated transducer was ~5.2 mm (acoustic NA=0.25) which is very close to the original target distance of 5.1 mm. PA and US pulse-echo resolutions in the focal zone were respectively ~55 µm and ~30 µm in the radial direction, and ~80 µm and ~60 µm in the transverse direction, but the transverse resolution showed variations according to target distance. Before forming the plastic acoustic lens, the original center frequency and fractional bandwidth of the transducer were determined to be ~41 MHz and 35% from pulse-echo measurements, however, it shifted down to ~37 MHz with a fractional bandwidth of 65% after affixing the acoustic lens. The transducer's housing diameter was 3.0-mm and had a 0.5-mm diameter hole along its central axis. The hole provides a conduit to route an optical fiber for light delivery. An advantage of using such plastic acoustic lens is that it also can serve as an acoustic matching layer to the crystal because its acoustic impedance is between that of the crystal and background water media.

2.2. Imaging test with a photoacoustic endoscopic probe

We tested the fabricated ultrasonic transducer with a PA endoscopic probe. **Figure 4** shows a schematic of the distal end of the endoscopic probe utilized for the imaging test. Laser pulses (584 nm, ~0.3 mJ/pulse) from an engaged laser system were guided by an optical fiber and emitted through the central hole of the single element ultrasonic transducer. After exiting the fiber, the laser beams are then directed by a reflector (or scanning mirror) towards the target and eventually generate PA waves once absorbed by the target tissue. The generated PA waves that propagate to the scanning mirror are reflected by the same mirror, sent to the transducer and finally converted into electric signals, which are digitally recorded by a computer. The scanning mirror steers both the light beam and the PA waves. It is important to note that the scanning mirror exhibits total internal acoustic reflection within the acceptance angles of the ultrasonic transducer and inserts no additional propagation losses into the ultrasonic detection because water and glass have a large ratio of sound propagation speeds (1.5/5.1, longitudinal wave; 1.5/3.3, shear wave).

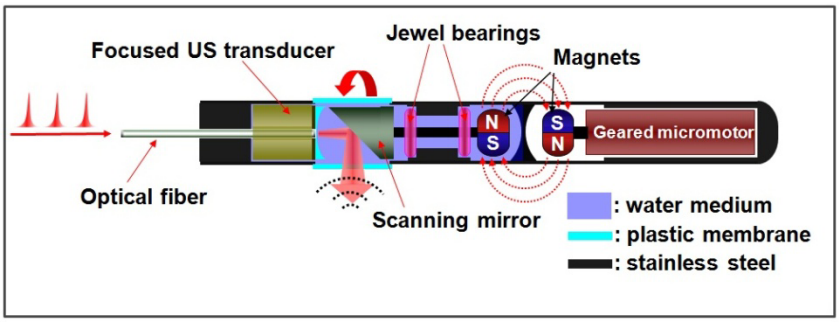

Figure 4. Schematic of the photoacoustic endoscopic probe.

The transducer and scanning mirror are housed under de-ionized water medium for acoustic impedance matching, and sealed with an optically and acoustically transparent, ~40 µm thick plastic membrane. All elements are encapsulated in a stainless steel streamline-shaped tube which allows for smooth intracavitary advancement. The optical fiber, the transducer's signal wires, and the micromotor's wires are also catheterized in a flexible PET plastic tube having ~1 m length. The probe's proximal body can be bent easily (more than 180° at the radius of curvature ~2 cm). More information on the endoscope's structure is available in our previous reports[2,3].

We imaged the upper esophagus of an adult New Zealand white rabbit *ex vivo* to test the focused transducer with real biological tissue. The rabbit was euthanized by an overdose of sodium pentobarbital (150 mg/kg) and the esophagus was filled with water for acoustic coupling. Then, we inserted the endoscopic probe into the esophagus ~20 cm deep from the animal's mouth and performed pullback volumetric scans over a ~6 cm range during constant pullback translation of the probe at a speed of ~100 µm/s. Each image required a scanning time of ~10 min. About 2800 B-scan slices with a longitudinal spacing of ~50 µm were acquired for the PA volumetric image. B-scan acquisition rate was about 2 Hz. For both PA and US imaging, the radial imaging depth was ~4.6 mm from the endoscope's surface, and the angular field-of-view (FOV) was approximately 270°, due to partial blocking of the probe housing. All procedures in the experiment followed the protocol approved by the Institutional Animal Care and Use Committee at Washington University in St. Louis.

3. RESULTS

In **Figure 5(a)**, we present a three-dimensional PA structural image from the rabbit's esophagus *ex vivo*, processed from a C-scan data set covering a cylindrical volume 6 cm long with a 13 mm diameter. The PA structural image was created from the PA data acquired at a 584 nm laser wavelength, in which the PA signal is only sensitive to the total hemoglobin concentration. The volume-rendered PA image shows the vasculature at the esophagus' wall and the tract's inner and outer boundaries having thickness of around 1 mm. A radial-maximum amplitude projection (MAP) image of (a) is shown in **Figure 5(b).** The MAP image enables straightforward comparison of organ sizes and positions between the three-dimensional endoscopy data and real anatomic structure after surgery.

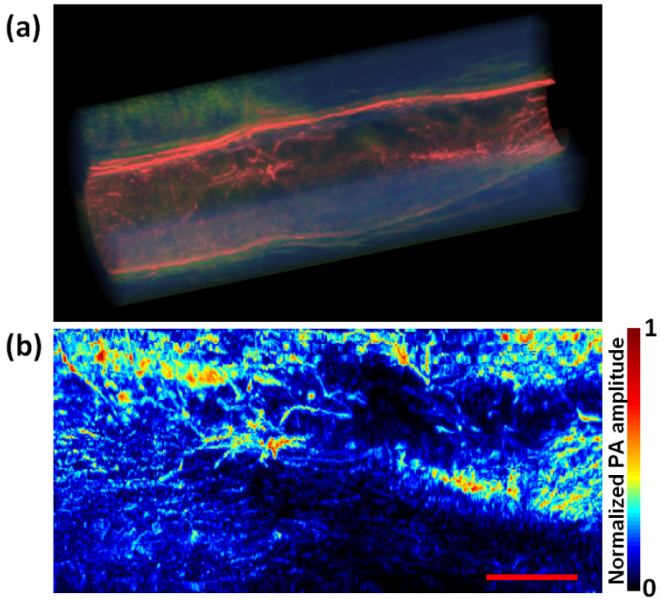

Figure 5. (a) Three-dimensionally-rendered PA structural image from a rabbit's esophagus acquired *ex vivo* over a 6 cm range with a 13 mm image diameter. The left-hand side and lower portion of the image correspond to the lower esophagus and the ventral side of the animal, respectively. **(b)** A PA radial-maximum amplitude projection image of (a). The upper and lower parts of each image correspond to the left and right sides of the animal, and the middle section of the images are from the ventral side of the rabbit. The dorsal side of the esophagus was not imaged due to the restricted angular FOV of the endoscope. The y-axis corresponds to the angular FOV covering 270° and the x-axis corresponds to pullback length of 6 cm. Scale bars represent 1 cm (only for the horizontal direction).

4. DISCUSSION

In PA endoscopic imaging, it is important to provide good acoustic matching condition to produce high quality volumetric images comparable to those from conventional ultrasonic imaging. Air bubbles or gaps between the endoscope and target organ can block acoustic wave transmission and will reduce the image quality. In this study, we could produce better three-dimensional vasculature images of the target tissue over a large scanning area by using water as the acoustic matching material rather than ultrasound gel, which was used in our previous *in situ* rat rectum imaging study[3]. The esophagus was imaged in situ over a cylindrical volume 6 cm long with a 13 mm diameter and a B-scan acquisition rate of 2 Hz. Most importantly, this study showed significant spatial resolution improvement of PA endoscopic image by employing a focused ultrasonic transducer.

ACKNOWLEDGEMENT

This work was sponsored in part by National Institutes of Health grants R01 CA157277, R01 NS46214 (BRP), R01 EB000712, R01 EB008085, and U54 CA136398 (Network for Translational Research). L.W. has a financial interest in Microphotoacoustics, Inc. and Endra, Inc., which, however, did not support this work. J.-M.Y. was supported in part by a Korea Research Foundation Grant funded by the Korean Government (KRF-2007-357-C00039).

REFERENCES

1. Wang, L.V. Prospects of photoacoustic tomography. *Med Phys* **35**, 5758-5767 (2008).
2. Yang, J.M*., et al.* Photoacoustic endoscopy. *Opt Lett* **34**, 1591-1593 (2009).
3. Yang, J.M*., et al.* Volumetric photoacoustic endoscopy of internal organs: a phantom and in situ study. in *Proc. SPIE*, Vol. 7564 75640D (2010).
4. Wang, L.V. Multiscale photoacoustic microscopy and computed tomography. *Nat Photonics* **3**, 503-509 (2009).
5. Wang, L.V. *(ed.) Photoacoustic Imaging and Spectroscopy*, (Taylor & Francis/CRC Press, 2009).
6. Oraevsky, A.A. & Karabutov, A.A. Optoacoustic Tomography. in *Biomedical Photonics Handbook*, Vol. PM125 (ed. Vo-Dinh, T.) 3401-3434 (CRC Press, 2003).
7. Chang, K.J., Nguyen, P., Erickson, R.A., Durbin, T.E. & Katz, K.D. The clinical utility of endoscopic ultrasound-guided fine-needle aspiration in the diagnosis and staging of pancreatic carcinoma. *Gastrointest Endosc* **45**, 387-393 (1997).
8. Menzel, J. & Domschke, W. Gastrointestinal miniprobe sonography: the current status. *Am J Gastroenterol* **95**, 605-616 (2000).
9. Tearney, G.J*., et al.* In vivo endoscopic optical biopsy with optical coherence tomography. *Science* **276**, 2037-2039 (1997).
10. Yun, S.H*., et al.* Comprehensive volumetric optical microscopy in vivo. *Nat Med* **12**, 1429-1433 (2006).
11. Kiesslich, R*., et al.* Confocal laser endoscopy for diagnosing intraepithelial neoplasias and colorectal cancer in vivo. *Gastroenterology* **127**, 706-713 (2004).
12. Min-Kang, C. & Sheng-Wen, C. Aspheric lens design. in *Ultrasonics Symposium, 2000 IEEE*, Vol. 2 1025-1028 vol.1022 (2000).
13. Maslov, K., Kinra, V.K. & Henderson, B.K. Elastodynamic response of a coplanar periodic layer of elastic spherical inclusions. *Mechanics of Materials* **32**, 785-795 (2000).